the Swiss-Norwegian Beamline (SNBL) at the European Synchrotron Radiation Facility in Grenoble according to Fig. 2. The method was first tested on a textured sample of the zeolite ZSM-5 ($[Si_{96}O_{192}]$·$4(C_3H_7)_4NOH$, space group *Pnma*, a = 20.049 Å, b = 19.933 Å, c = 13.390 Å) with 38 framework atoms in the asymmetric unit. Pole-figure data for eight single reflections and full diffraction patterns at four sample orientations were measured. As predicted, all four patterns displayed the same very high resolution independent of the tilt angle. A single set of reflection intensities was extracted from the four patterns with a modified Le Bail algorithm (*10*) and was used as input into a standard direct methods program. With default settings, all 12 Si positions and 19 of the 26 O positions were found in the top 40 peaks of the sharpened electron density map (E-map). With the improved reflection intensity data, this very complex structure could be solved in a routine manner.

The method was then applied to two materials with unknown structures. The first of these materials was the aluminophosphate molecular sieve Mu-9 (*11*). Like many materials, Mu-9 contained an unidentified impurity. This impurity not only made an accurate chemical analysis impossible but also created serious problems with the indexing of the powder pattern. However, the texture measurement allowed the peaks belonging to Mu-9 to be identified unambiguously and the pattern to be indexed satisfactorily (space group $R\bar{3}c$, a = 14.057 Å and c = 42.295 Å). Intensity extraction (six pole figures and five full patterns) followed by the application of direct methods then revealed an unexpected framework composition ($[Al_{66}P_{72}O_{288}]^{18-}$) and an unusual structure with 13 framework atoms in the asymmetric unit. One of the three Al atoms proved to be (unexpectedly) six- rather than four-connected to framework P atoms.

The second material of unknown structure was the zeolite UTD-1 (*12*) prepared with a modification of the published synthesis procedure (*13*). In contrast to the body-centered orthorhombic unit cell reported for calcined UTD-1 (a = 18.98 Å, b = 8.41 Å, c = 23.04 Å) (*14*), the diffraction pattern of this as-synthesized material could only be indexed with a primitive monoclinic cell (a = 14.9633 Å, b = 8.4704 Å, c = 30.0098 Å, β = 102.667°). Furthermore, no evidence of faulting, which was reported for the calcined form, could be discerned. These observations indicated that the material might be substantially different from that of Lobo and coworkers (*14*), and further investigation seemed to be warranted.

The needle-like crystals were aligned with shear forces in a polystyrene matrix. Pole-figure data for seven reflections and full diffraction patterns at five sample orientations were measured (Fig. 3). Application of direct methods to the reflection intensities extracted assuming the space group $P2_1/c$ produced an E-map with 16 Si atoms, which described a complete three-dimensional, four-connected framework with 14-ring pores [related to polymorph C in (*14*)]. Seventeen of the bridging O atoms were also found on that initial E-map. Difference electron density maps allowed the remaining 15 O atoms, the (nonframework) Co, and the pentamethylcyclopentadienyl rings to be located. Subsequent Rietveld refinement showed the correct space group to be noncentrosymmetric (*Pc*) with 117 atoms in the asymmetric unit (Fig. 4). The Co complex is fully ordered in the 14-ring channels.

The determination of such a complex structure (69 non-H atoms in the asymmetric unit in $P2_1/c$) from powder diffraction data with standard crystallographic methods provides a clear demonstration of the power of the texture approach. The method can be applied to any class of compounds, and the only requirement is that a sample with preferred orientation can be prepared. This is generally possible with one of the many known techniques. A larger range of structural complexity hereby becomes accessible to scientists interested in the structures of polycrystalline materials that cannot be grown as single crystals.

References and Notes

1. J. Jansen, R. Peschar, H. Schenk, *Z. Kristallogr.* **206**, 33 (1993); C. Giacovazzo, *Acta Crystallogr. Sect. A* **52**, 331 (1996); C. J. Gilmore, K. Henderson, G. Bricogne, *ibid.* **47**, 830 (1991); H. Gies and J. Rius, *Z. Kristallogr.* **210**, 475 (1995).
2. M. W. Deem and J. M. Newsam, *J. Am. Chem. Soc.* **114**, 7189 (1992); R. W. Grosse-Kunstleve, L. B. McCusker, C. Baerlocher, *J. Appl. Crystallogr.* **30**, 985 (1997); K. Shankland, W. I. F. David, T. Csoka, *Z. Kristallogr.* **212**, 550 (1997); K. D. M. Harris, R. L. Johnston, B. M. Kariuki, *Acta Crystallogr. Sect. A* **54**, 632 (1998); Y. G. Andreev, P. Lightfoot, P. G. Bruce, *J. Appl. Crystallogr.* **30**, 294 (1997); Y. G. Andreev and P. G. Bruce, *Mater. Sci. Forum* **278-281**, 14 (1998).
3. W. I. F. David, *J. Appl. Crystallogr.* **20**, 316 (1987); *Nature* **346**, 731 (1990); J. Jansen, R. Peschar, H. Schenk, *J. Appl. Crystallogr.* **25**, 237 (1992); M. A. Estermann and V. Gramlich, *ibid.* **26**, 396 (1993); D. S. Sivia and W. I. F. David, *Acta Crystallogr. Sect. A* **50**, 703 (1994); A. Altomare *et al.*, *J. Appl. Crystallogr.* **31**, 74 (1998).
4. W. Lasocha and H. Schenk, *J. Appl. Crystallogr.* **30**, 561 (1997).
5. K. Shankland, W. I. F. David, D. S. Sivia, *J. Mater. Chem.* **7**, 569 (1997).
6. A. Altomare, G. Cascarano, C. Giacovazzo, A. Guagliardi, *J. Appl. Crystallogr.* **27**, 1045 (1994); R. Peschar, H. Schenk, P. Capkova, *ibid.* **28**, 127 (1995).
7. R. Hedel, H. J. Bunge, G. Reck, *Textures Microstructures* **29**, 103 (1997).
8. H.-J. Bunge, *Texture Analysis in Materials Science* (Cuvillier Verlag, Göttingen, Germany, 1993).
9. J. B. Hastings, W. Thomlinson, D. E. Cox, *J. Appl. Crystallogr.* **17**, 85 (1984).
10. A. Le Bail, H. Duroy, J. L. Fourquet, *Mater. Res. Bull.* **23**, 447 (1988).
11. T. Wessels, L. Yu, J.-L. Guth, A. Matijasic, in preparation.
12. C. C. Freyhardt, M. Tsapatsis, R. F. Lobo, K. J. Balkus, M. E. Davis, *Nature* **381**, 295 (1996).
13. T. Wessels, C. Baerlocher, L. B. McCusker, E. J. Creyghton, in preparation.
14. R. F. Lobo *et al.*, *J. Am. Chem. Soc.* **119**, 8474 (1997).

15. We thank the SNBL for allowing us access to their synchrotron facility and P. Pattison for his assistance with the experimental setup. Supported by the Swiss National Science Foundation.

3 November 1998; accepted 9 March 1999

Synergistic Signaling in Fetal Brain by STAT3-Smad1 Complex Bridged by p300

Kinichi Nakashima,[1,2] Makoto Yanagisawa,[1] Hirokazu Arakawa,[1] Naoki Kimura,[1] Tatsuhiro Hisatsune,[3] Masahiro Kawabata,[4] Kohei Miyazono,[4] Tetsuya Taga[1]*

The cytokines LIF (leukemia inhibitory factor) and BMP2 (bone morphogenetic protein–2) signal through different receptors and transcription factors, namely STATs (signal transducers and activators of transcription) and Smads. LIF and BMP2 were found to act in synergy on primary fetal neural progenitor cells to induce astrocytes. The transcriptional coactivator p300 interacts physically with STAT3 at its amino terminus in a cytokine stimulation–independent manner, and with Smad1 at its carboxyl terminus in a cytokine stimulation–dependent manner. The formation of a complex between STAT3 and Smad1, bridged by p300, is involved in the cooperative signaling of LIF and BMP2 and the subsequent induction of astrocytes from neural progenitors.

Interleukin (IL)–6 and the five related cytokines IL-11, LIF, ciliary neurotrophic factor, oncostatin M, and cardiotrophin-1 share the membrane glycoprotein gp130 as a receptor component critical for signal transduction (*1*). These six IL-6–type cytokines trigger the dimerization of gp130, activating associated cytoplasmic tyrosine kinases in the Janus ki-

nase family and a downstream transcription factor, STAT3 (*1*). BMPs and related members of the transforming growth factor (TGF)–β superfamily signal through heterotetrameric serine-threonine kinase receptors (*2*). Activated BMP receptors phosphorylate transcription factors Smad1, 5, or 8, which in turn associate with a common mediator, Smad4. The resultant heteromeric Smad complexes then translocate into the nucleus to regulate transcription (*2*).

Using the cultures of fetal neuroepithelial cells that are considered to contain neural precursors (*3–5*), we found that LIF and BMP2 function in synergy to induce differentiation into astrocytes (*6, 7*) (Fig. 1). Astrocytes were identified by expression of an astrocyte marker, glial fibrillary acidic protein (GFAP). BMP2 or LIF alone (up to 200 ng/ml) did not induce astrocyte development. BMP4 combined with IL-6 plus soluble IL-6 receptor (sIL-6R) also promoted astrocyte development (*8*).

To investigate a molecular mechanism of the synergism, we first examined the transcription factors activated by these cytokines. Smad6 may repress TGF-β and BMP signaling by inhibiting receptor-mediated phosphorylation of signal-specific Smad species or competing with them for binding with the regulatory Smad4 (*9, 10*). Transfection with this inhibitory Smad, Smad6, reduced the promoter activation induced by BMP2 and by a combination of BMP2 and LIF, but not by LIF alone (*6, 11*) (Fig. 2A). Smad7, another inhibitor of Smad signaling, also suppressed promoter activation by a BMP2-LIF combination almost to the level induced by LIF alone (*8*). Overexpression of a dominant negative form of STAT3 (DN-STAT3) inhibited GFAP promoter activation by LIF and by a BMP2-LIF combination. Although the inhibition was not complete, these results suggest that activation of both Smads and STAT3 by relevant cytokines is required for the synergistic effect of BMP2 and LIF on astrocyte differentiation.

We constructed mutations in the GFAP gene promoter to identify regions required for effects of LIF and BMP2 on the promoter. A single STAT3 binding site (TTCCGAGAA) is required for rat GFAP promoter activation by IL-6 family cytokines (*5*). This sequence, conserved in the mouse GFAP promoter, is located between nucleotide positions –1518 and –1510 (*12*). When the STAT3 binding site was deleted (GF1L-S-pGL3), responsiveness to LIF and to a combination of LIF and BMP2 was reduced (*6, 11*) (Fig. 2B). Residual GFAP promoter activation with this construct might be attributable to one remaining putative STAT3 binding site (TTACCAGAA) that is also conserved between mouse and rat (marked by a dot in Fig. 2B, left panel) (*12, 13*). The deletion also caused reduction in BMP2 response, implying that the deleted region interacts with Smad proteins. Appending the STAT3 binding element at the 5′ end of this deleted construct (SBSW-GF1L-SB-pGL3) restored the response to LIF and the synergistic response to LIF and BMP2. A larger deletion (GF1L-K-pGL3) abolished BMP2 responsiveness with or without LIF. Thus, the deleted fragment contains another region required for BMP2 response. Responsiveness to both LIF and BMP2—mediated by STAT3 and Smads, respectively—is required for the synergism between LIF and BMP2. The consensus binding sequence for Smad3 and Smad4 is 5′-AG(C/A)CAGACA-3′ (*14*) or 5′-GTCTAGAC-3′ (*15*), and the latter may be capable of binding

[1]Department of Molecular Cell Biology, [2]Cell Fate Modulation Research Unit, Medical Research Institute, Tokyo Medical and Dental University, Tokyo 101-0062, Japan. [3]Department of Applied Biological Chemistry, University of Tokyo, Tokyo 113-8857, Japan. [4]Department of Biochemistry, Cancer Institute, Japanese Foundation for Cancer Research, and Research for the Future Program, Japan Society for the Promotion of Science, Tokyo 170-8455, Japan.

*To whom correspondence should be addressed. E-mail: tagamcb@mri.tmd.ac.jp

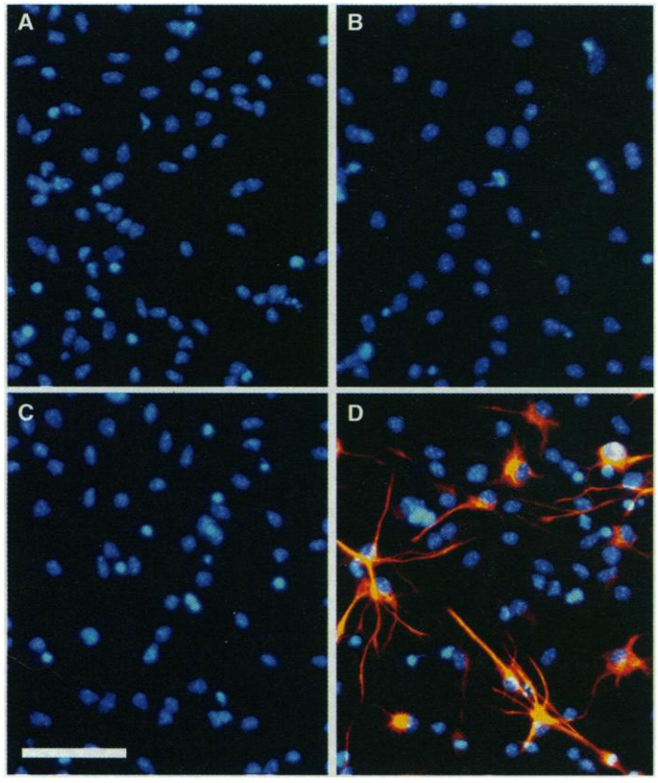

Fig. 1. Synergistic enhancement of astrocyte differentiation from neuroepithelial cells by BMP2 and LIF. Cells were cultured with medium alone (**A**), BMP2 (80 ng/ml) (**B**), LIF (80 ng/ml) (**C**), or BMP2 (80 ng/ml) plus LIF (80 ng/ml) (**D**), and subjected to immunofluorescent staining for GFAP. Scale bar, 50 μm.

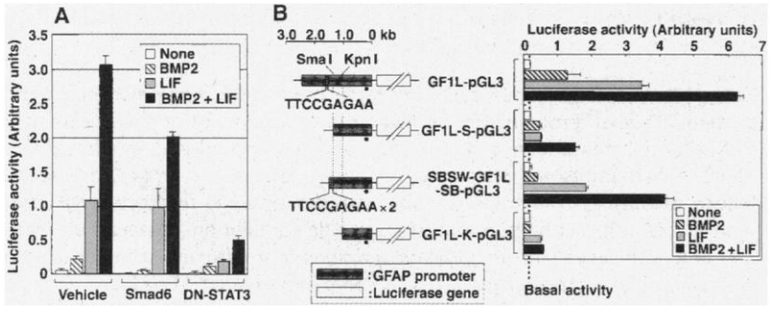

Fig. 2. Smads and STAT3 are both required for synergism between BMP2 and LIF. (**A**) Neuroepithelial cells were cotransfected with GF1L-pGL3 and R-Luc along with control vehicle or a construct expressing Smad6 or DN-STAT3, and then stimulated with the indicated cytokines. (**B**) Neuroepithelial cells were transfected with GF1L-pGL3 or modified versions of reporter constructs along with R-Luc (left panel); the locus of the proximal potential STAT3 binding site conserved between mouse and rat is marked by large dots below the bars representing GFAP promoters. The cells were then treated with each cytokine as indicated (right panel).

to Smad1 as well (*16*). The GFAP gene promoter has no identical sequence but has three similar sequences: 5′-CAGAGA-3′ at positions −1406 to −1401, 5′-GAGTAGACA-3′ at −1373 to −1365, and 5′-GACACA-3′ at −1290 to −1285. However, even though nucleotide substitutions were introduced in all three sequences simultaneously, no significant reduction in the response of the reporter construct to BMP2 and a combination of BMP2 and LIF was observed (*8*). This implies that an unidentified nucleotide sequence exists that may contribute to Smad-mediated GFAP promoter activation.

STAT3 and one or more Smads may physically interact to promote the synergy between LIF and BMP2 in astrocyte differentiation. We were unable to detect such interaction in COS-7 cells overexpressing STAT3 and Smad1, even after cells were stimulated with a combination of IL-6 and sIL-6R and coexpression of constitutively active type I BMP receptor (CA-ALK3) (*8*). We thus hypothesized that STAT3 and Smad1 may interact via an adaptor molecule. The CREB-binding protein (CBP)/p300 family of transcriptional coactivators interacts with various transcription factors such as AP-1, Myb, and nuclear receptors, altering their activity (*17*). Smad1, 2, 3, and 4 associate with CBP/p300 family members (*18, 19*), and STAT1, 2, and 5 also associate with them (*20*). As shown in Fig. 3, p300 was detected in the immune complex of Smad1 when cells were stimulated by coexpression of CA-ALK3 (Fig. 3A) and in the STAT3 immune complex independent of IL-6 stimulation (Fig. 3B) (*21*). These results imply that p300 acts as an adaptor molecule that links Smad1 and STAT3. Smad1 was present in the STAT3 immune complex only in the presence of p300 in a CA-ALK3 stimulation–dependent manner (Fig. 3C), confirming the p300-mediated complex formation of activated Smad1 and STAT3. Exogenously expressed p300 enhanced the GFAP promoter activation induced by each cytokine alone as well as in combination (*6, 11*) (Fig. 3D). We suggest that p300 bridges STAT3 and Smad1 proteins, leading to synergistic transcriptional activation of the GFAP promoter.

To understand the mechanism of p300-mediated association of STAT3 and Smad1 in more detail, we determined what regions in the p300 protein were important for interaction with Smad1 and STAT3 (*21*). In the presence of CA-ALK3, Smad1 interacted most with a COOH-terminal fragment of p300 spanning amino acid residues 1737 to 2414 [p300(1737–2414)] (Fig. 4A), as indicated for other Smad species (*18*). Weaker Smad1 association was observed with p300(1–682) and p300(1–1030) mutants. A p300(1–1736) protein species failed to interact with Smad1, which implies that the region between residues 1030 and 1736 may inhibit the interaction by masking the NH_2-terminally located interaction domain. STAT3 associated most with two NH_2-terminal p300 fragments, p300(1–682) and p300(1–1030) (Fig. 4B). The p300(1–1736) fragment bound neither STAT3 nor Smad1. The association of STAT3 with the COOH-terminal p300 fragment, p300(1737–2414), was much weaker than with the two NH_2-terminal fragments. Thus, it is likely that the NH_2-terminal portion of p300 interacts with STAT3 and the COOH-terminal portion with Smad1. The complex of STAT3, Smads, and p300 contributes to the LIF- and BMP2-mediated GFAP promoter activation, and truncated forms of p300 should

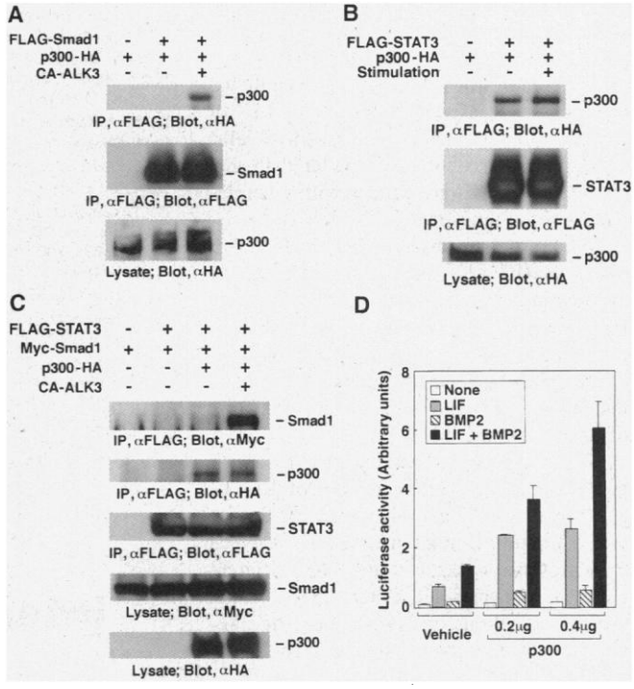

Fig. 3. STAT3 and Smad1 proteins are bridged by p300, leading to synergistic transcriptional activation of the GFAP promoter. (**A**) HA-tagged p300 was transfected into COS-7 cells with FLAG-tagged Smad1 and HA-tagged CA-ALK3 constructs (*9*). Cell extracts were subjected to immunoprecipitation (IP) with anti-FLAG (αFLAG). Precipitates or lysates were separated by SDS-PAGE and analyzed by immunoblotting with anti-HA (αHA). Expression of Smad1 and p300 was monitored. (**B**) HA-tagged p300 was expressed together with FLAG-tagged STAT3 (*23*) in COS-7 cells. The cells were stimulated with a combination of IL-6 (100 ng/ml) and sIL-6R (200 ng/ml) for 15 min. Cell extracts were immunoprecipitated with anti-FLAG and analyzed by SDS-PAGE followed by immunoblotting with anti-HA. Expression of p300 and STAT3 is shown. (**C**) Myc-tagged Smad1 was expressed together with FLAG-tagged STAT3, HA-tagged p300, and CA-ALK3 in COS-7 cells. Cell extracts were immunoprecipitated with anti-FLAG and then subjected to immunoblotting with the indicated antibodies. Comparable expression of Smad1 and STAT3 is indicated. (**D**) Neuroepithelial cells were transfected with the indicated concentrations (per milliliter) of p300 expression construct together with reporter and control plasmids. The transfected cells were stimulated with cytokines (80 ng/ml) separately or in combination, as indicated. Control vehicle was used to adjust the total amount of DNA used in each transfection.

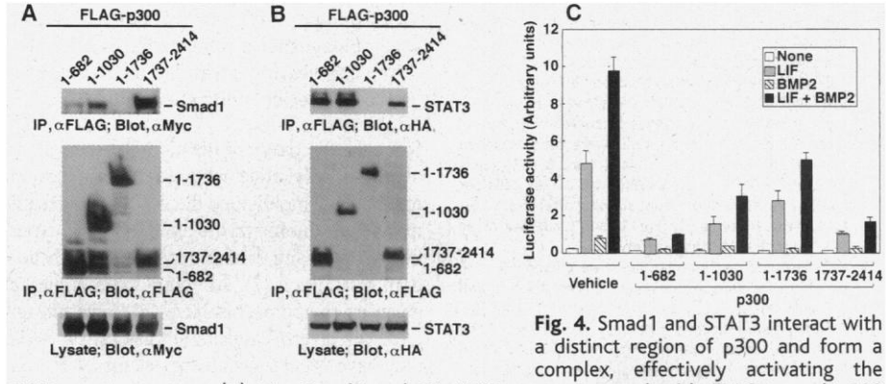

Fig. 4. Smad1 and STAT3 interact with a distinct region of p300 and form a complex, effectively activating the GFAP gene promoter. (**A**) Myc-Smad1 and CA-ALK3 were expressed with FLAG-tagged p300 fragments as indicated. Lysates were immunoprecipitated with anti-FLAG, and the precipitates were analyzed by protein immunoblotting with anti-Myc. (**B**) HA-STAT3 expression construct was transfected into COS-7 cells with FLAG-tagged p300 fragment expression constructs as depicted. Immunoprecipitation was performed with anti-FLAG and then analyzed by immunoblotting with anti-HA. (**C**) Respective truncated p300 constructs were cotransfected with reporter and control plasmids into neuroepithelial cells as indicated. The cells were stimulated with cytokines (80 ng/ml) separately or in combination, as depicted.

impede the GFAP promoter activation by the two cytokines. Expression of any of the p300 deletion mutants used in this experiment reduced the GFAP promoter activation by LIF and BMP2 either alone or in combination (*6, 11*) (Fig. 4C), possibly by competing with the endogenous p300 for the binding to STAT3 and Smad1. The p300(1–1736) fragment, which interacted with neither STAT3 nor Smad1, also behaved as an inhibitor, possibly because of the seclusion of downstream targets of endogenous p300.

It is interesting that the neuroepithelial cell cultures (*6*) over 3 days with LIF or BMP2 alone produced GFAP-positive cells, although their extent was smaller than that observed in the 2-day culture with a combination of LIF and BMP2 (*8*). This is consistent with previous observations in which LIF (*5*) or BMP2 (*22*) alone induced astrocyte differentiation in cultures for a relatively longer period. This may be due to the formation of a STAT3-Smad1-p300 complex induced by an exogenously added cytokine and the endogenous expression and accumulation of its counterpart.

We have proposed a mechanism by which p300 coordinates the interaction of STAT3 and Smad1, leading to synergistic astrocyte differentiation. Similar interactions between transcriptional coactivators and different kinds of transcription factors may explain synergistic actions of distinct types of cytokines in other biological signaling pathways.

References and Notes

1. T. Taga and T. Kishimoto, *Annu. Rev. Immunol.* **15**, 797 (1997).
2. C.-H. Heldin, K. Miyazono, P. ten Dijke, *Nature* **390**, 465 (1997); R. Derynck, Y. Zhang, X.-H. Feng, *Cell* **95**, 737 (1998).
3. K. K. Johe, T. G. Hazel, T. Muller, M. M. Dugich-Djordjevic, R. D. G. McKay, *Genes Dev.* **10**, 3129 (1996); P. Rajan and R. D. G. McKay, *J. Neurosci.* **18**, 3620 (1998).
4. R. McKay, *Science* **276**, 66 (1997).
5. A. Bonni *et al.*, *ibid.* **278**, 477 (1997).
6. Neuroepithelial cells were prepared from embryonic day 14 mouse telencephalons as described (*3, 5*). Initially, plated cells were expanded for 4 days in N2-supplemented Dulbecco's modified Eagle's medium (DMEM)/F12 containing 10 ng/ml of basic fibroblast growth factor on dishes precoated with poly-L-ornithine and fibronectin. Cells were then detached and replated on Chamber Slides (Nunc; 8×10^4 cells per well) or 24-well plates (Nunc; 6×10^5 cells per well) for immunofluorescent staining after 2-day culture with cytokines (*7*) (Fig. 1) and luciferase assay (*11*) (Figs. 2 to 4), respectively.
7. Cells cultured on Chamber Slides were fixed with 4% paraformaldehyde in phosphate-buffered saline and stained with antibody to GFAP (Dako) and rhodamine-conjugated second antibody (Chemicon). The cells were counterstained with Hoechst 33258 to identify nuclei. Images were obtained using fluorescent microscopy (AX70, Olympus).
8. K. Nakashima and T. Taga, unpublished data.
9. T. Imamura *et al.*, *Nature* **389**, 622 (1997).
10. A. Hata, G. Lagna, J. Massagué, A. Hemmati-Brivanlou, *Genes Dev.* **12**, 186 (1998).
11. Neuroepithelial cells were transfected with a luciferase reporter gene fused with the 2.5-kb GFAP promoter (GF1L-pGL3) (Figs. 2 to 4) or its modified versions (GF1L-S-pGL3, SBSW-GF1L-SB-pGL3, or GF1L-K-pGL3) (Fig. 2) using Trans-IT LT-1 (Mirus) according to the manufacturer's protocol. As an internal control, a plasmid containing sea pansy luciferase expression construct was cotransfected. The following expression constructs were also used: DN-STAT3 (*23*) and Smad6 (*9*) in pEF-BOS (*24*) (Fig. 2), full-length p300 in CMV-β (18) (Fig. 3), and fragments of p300 (1–682, 1–1030, 1–1736, and 1737–2414) in pcDEF3 (*18*) (Fig. 4). On the following day, cells were stimulated with each cytokine (80 ng/ml) for 8 hours and solubilized. Luciferase activity was measured according to the recommended procedures for the Pikkagene Dual Luciferase Assay System (Toyo Ink Inc.). Luminous CT-9000D (Dia-Iatron) was used for quantitation.
12. M. Miura, T. Tamura, K. Mikoshiba, *J. Neurochem.* **55**, 1180 (1990).
13. M. A. Kahn *et al.*, *ibid.* **68**, 1413 (1997).
14. S. Dennler *et al.*, *EMBO J.* **17**, 3091 (1998).
15. L. Zawel *et al.*, *Mol. Cell* **1**, 611 (1998).
16. Y. Shi *et al.*, *Cell* **94**, 585 (1998).
17. Y. Kamei *et al.*, *ibid.* **85**, 403 (1996); P. Dai *et al.*, *Genes Dev.* **10**, 528 (1996); R. Kurokawa *et al.*, *Science* **279**, 700 (1998); J. C. Chrivia *et al.*, *Nature* **365**, 855 (1993).
18. A. Nishihara *et al.*, *Genes Cells* **3**, 613 (1998).
19. R. Janknecht, N. J. Wells, T. Hunter, *Genes Dev.* **12**, 2114 (1998); X.-H. Feng, Y. Zhang, R.-Y. Wu, R. Derynck, *ibid.*, p. 2153; C. Pouponnot, L. Jayaraman, J. Massagué, *J. Biol. Chem.* **273**, 22865 (1998); J. N. Topper *et al.*, *Proc. Natl. Acad. Sci. U.S.A.* **95**, 9506 (1998).
20. J. J. Zhang *et al.*, *Proc. Natl. Acad. Sci. U.S.A.* **93**, 15092 (1996); S. Bhattacharya *et al.*, *Nature* **383**, 344 (1996); E. Pfitzner, R. Jähne, M. Wissler, E. Stoecklin, B. Groner, *Mol. Endocrinol.* **12**, 1582 (1998).
21. COS-7 cells were maintained in DMEM containing 10% fetal bovine serum and transfected with expression constructs using Trans-IT LT-1. After 24 to 36 hours of culture, cells were solubilized as described (*25*). Lysates were immunoprecipitated with antibodies to FLAG (Sigma) or to hemagglutinin (HA) (Santa Cruz). Precipitates and, in some cases, cell lysates were subjected to SDS–polyacrylamide gel electrophoresis (PAGE) followed by immunoblotting with anti-FLAG, anti-HA, or anti-Myc (Genosys).
22. R. E. Gross *et al.*, *Neuron* **17**, 595 (1996).
23. M. Minami *et al.*, *Proc. Natl. Acad. Sci. U.S.A.* **93**, 3963 (1996).
24. S. Mizushima and S. Nagata, *Nucleic Acids Res.* **18**, 5322 (1990).
25. K. Nakashima, M. Narazaki, T. Taga, *FEBS Lett.* **401**, 49 (1997).

26. We thank R. Eckner for HA-p300, M. Minami and S. Akira for DN-STAT3, K. Shimozaki and S. Nagata for pEF-BOS and R-Luc, K. Ikenaka for GFAP gene promoter, K. Yasukawa for sIL-6R, Genetics Institute for BMP2 and BMP4, A. Nishihara for p300 deletion constructs, J. Akai and R. Hata for help and discussion on luciferase assays, and T. Imamura for valuable discussion. We also thank Y. Nakamura for secretarial assistance and K. Saito for technical help. Supported by a grant-in-aid from the Ministry of Education, Science, Sports and Culture of Japan and by the Human Frontier Science Program, Cell Science Research Foundation, and Kowa Life Science Foundation.

15 December 1998; accepted 4 March 1999

Dissecting and Exploiting Intermodular Communication in Polyketide Synthases

Rajesh S. Gokhale,[1] Stuart Y. Tsuji,[1] David E. Cane,[4] Chaitan Khosla[1,2,3]*

Modular polyketide synthases catalyze the biosynthesis of medicinally important natural products through an assembly-line mechanism. Although these megasynthases display very precise overall selectivity, we show that their constituent modules are remarkably tolerant toward diverse incoming acyl chains. By appropriate engineering of linkers, which exist within and between polypeptides, it is possible to exploit this tolerance to facilitate the transfer of biosynthetic intermediates between unnaturally linked modules. This protein engineering strategy also provides insights into the evolution of modular polyketide synthases.

Since the discovery of the modular architecture of certain polyketide synthases (PKSs), several reports have highlighted the functional versatility of these multienzyme assemblies by experiments involving domain inactivation, substitution, or addition (*1*). Although these empirical gene fusion approaches have led to the biosynthesis of diverse "unnatural" natural products, they have usually resulted in decreased in vivo productivity (*2*). The reasons for the lower productivity are poorly understood but could include structural instability of the engineered protein, suboptimal chemistry within the altered module, or inefficient processing of the nonnatural polyketide intermediates by downstream modules.

An alternative strategy for combinatorial biosynthesis would be to recombine intact modules from the vast natural repertoire of PKSs. Such an approach would benefit from the use of highly evolved modules as intact catalytic units, thereby eliminating unwanted perturbations in module structure or chemistry. Along with the diverse chemistry observed in polyketide biosynthetic pathways, greater degrees of freedom

[1]Department of Chemical Engineering, [2]Department of Chemistry, [3]Department of Biochemistry, Stanford University, Stanford CA 94305–5025, USA. [4]Department of Chemistry, Brown University, Box H, Providence RI 02912–9108, USA.

*To whom correspondence should be addressed.